

Supplementary Information

Rock Salt Type α -MnS Anode for High-Rate Sodium Storage

Chang-Heum Jo, Ji-Ung Choi and Seung-Taek Myung *

*Department of Nano Technology and Advanced Materials Engineering & Sejong
Battery Institute, Sejong University, Gunja-dong, Gwangjin-gu, Seoul 05006, South
Korea*

*Corresponding author

E-mail: smyung@sejong.ac.kr (S. Myung)

Table S1. Recent progress of MX / Na battery (M: transition metal).

Material	Synthesis method	Voltage range (V)	First charge capacity (mAh g ⁻¹ (A g ⁻¹))	Capacity (mAh g ⁻¹) after (x) cycle	Coulombic efficiency of first cycle (%)	Electrolyte	ref
C- α -MnS	Solvothermal	0-3	302 (0.1)	272 (200)	75	0.5M NaPF ₆ in PC + 2%FEC	This work
MnS microsphere/rGO	Hydrothermal	0.01-2.6	497(0.1)	308(125)	62	1M NaClO ₄ in EC/DEC (4:6) with 2% FEC	1
NiS ₂ /rGO	Microwave-assisted	0.005-3.0	418.7(0.1)	370.2(50)	70.5	1M NaClO ₄ in EC/PC (1:1) with 5% FEC	2
CoS ₂ /rGO	Solvothermal	0.01-3.0	231.5(0.5)	249(100)	39.2	1M NaClO ₄ in EC/PC (1:1) with 5% FEC	3
Co ₃ S ₄ /graphene	Anion exchange	0.005-3	423(0.5)	329(50)	53	1M NaClO ₄ in EC/PC (1:1) with 10% FEC	4
MoS ₂	Solvothermal	0-3	338(0.025)	240(20)	57	1M NaPF ₆ in EC+DMC with 2% FEC	5
MoS ₂ /graphene nanosheet	Commercialized	0.01-2.7	484(0.1)	432(60)	52	1M NaClO ₄ in EC/DMC (1:1)	6
TiO ₂ /C	Solvothermal	1-1.25	275(0.05)	150(10000)	55.9	1M NaClO ₄ in DMC/EC/EMC (1:1:1) with 5% FEC	7
TiO ₂ /C nanosheets	Hydrothermal	0.01-3	350(0.1)	264.9(100)	51.8	1M NaPF ₆ in DMC/EC/EMC (1:1:1)	8

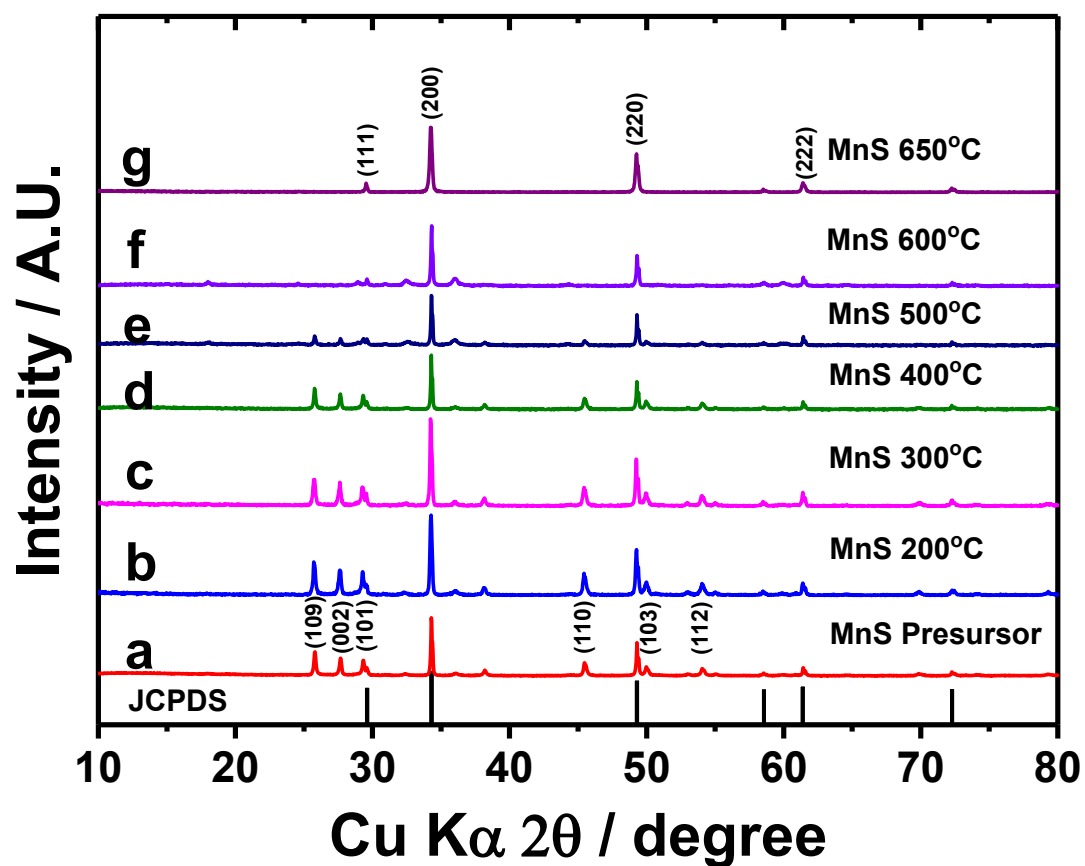


Figure S1. XRD patterns of as-synthesized products; (a) solvothermally produced γ -MnS, heat-treated γ -MnS under Ar stream at (b) 200 °C, (c) 300 °C, (d) 400 °C, (e) 500 °C, (f) 600 °C, and (f) 650 °C, at which single-phase α -MnS was formed.

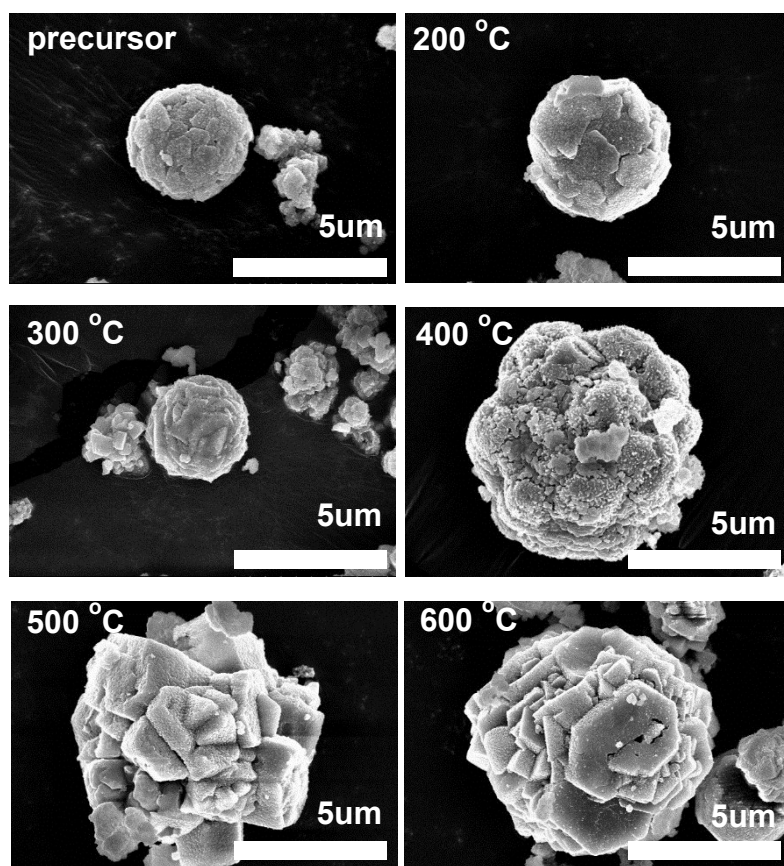


Figure S2. SEM images of as-synthesized products; (a) solvothermally produced γ -MnS, heat-treated γ -MnS under Ar stream at (b) 200 °C, (c) 300 °C, (d) 400 °C, (e) 500 °C, (f) 600 °C, and (f) 650 °C, at which single-phase α -MnS was formed.

Table S2. Rietveld refinement results of the bare and carbon-coated α -MnS.

Bare MnS						
Atom	Site	x	y	z	g	B/Å
Mn	4a	0	0	0	1	0.5
S	4b	0.5	0.5	0.5	1	1.1
Cell parameters				a=b=c= 5.2223(5) Å		
Rp (%) : 9.8 , Rwp (%) : 13.2						
Black MnS						
Atom	Site	x	y	z	g	B/Å
Mn	4a	0	0	0	1	0.5
S	4b	0.5	0.5	0.5	1	1.1
Cell parameters				a=b=c= 5.2221(2) Å		
Rp (%) : 7.1 , Rwp (%) : 12.3						

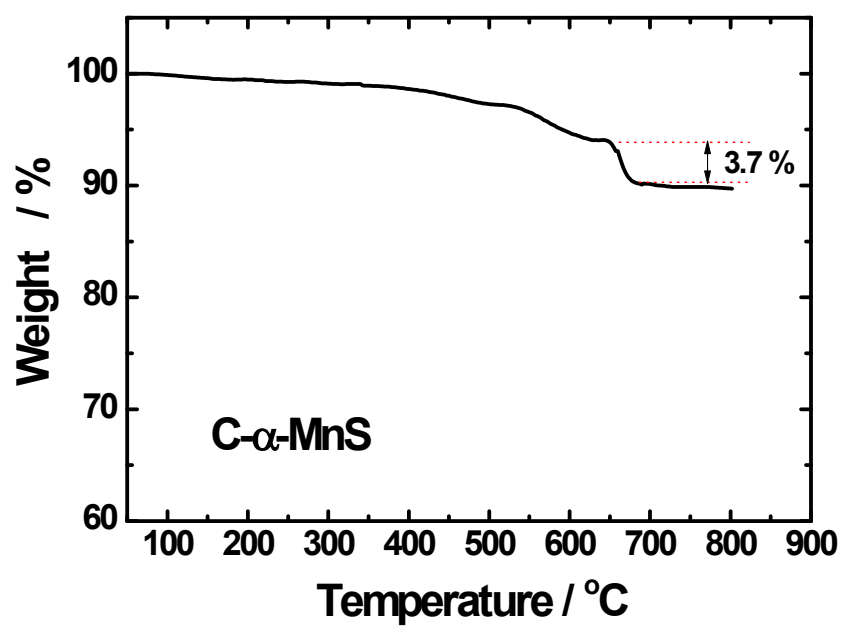


Figure S3. TGA curves of C- α -MnS measured in air.

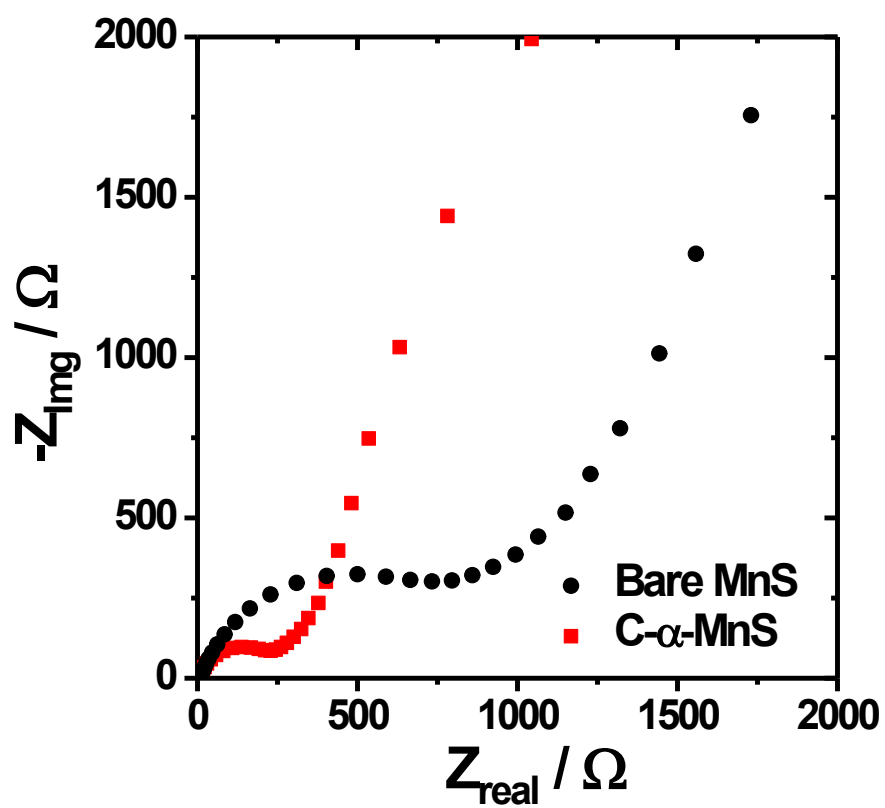


Figure S4. Cole–Cole plots of fresh bare and carbon-coated α -MnS electrodes.

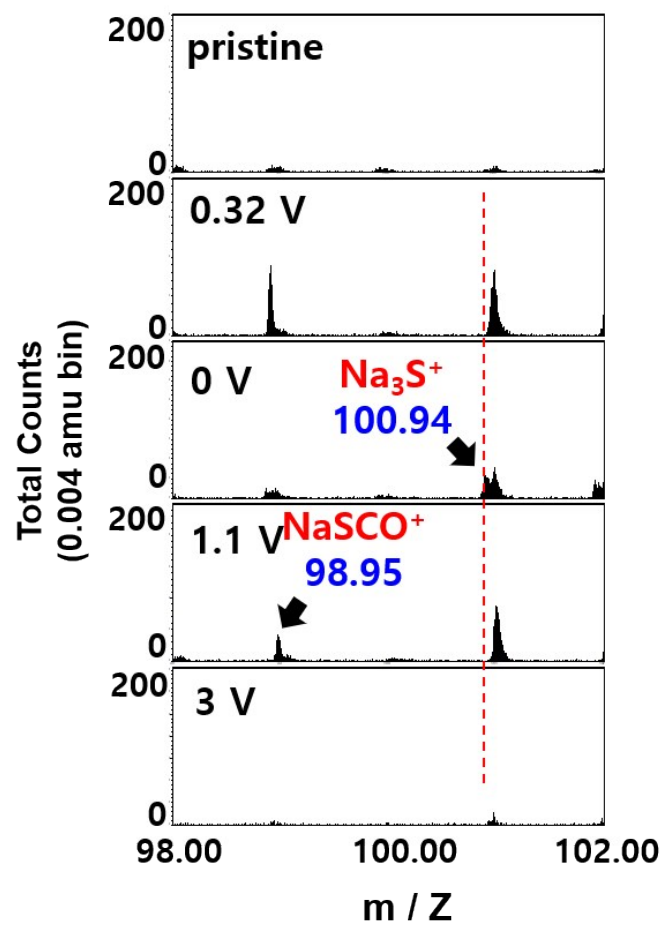


Figure S5. ToF-SIMS spectra of the C- α -MnS electrode upon sodiation (reduction) and de-sodiation (oxidation), left: NaSCO_2^+ positive fragment ($m=98.95$) and Na_2S^+ positive fragment ($m=100.94$).

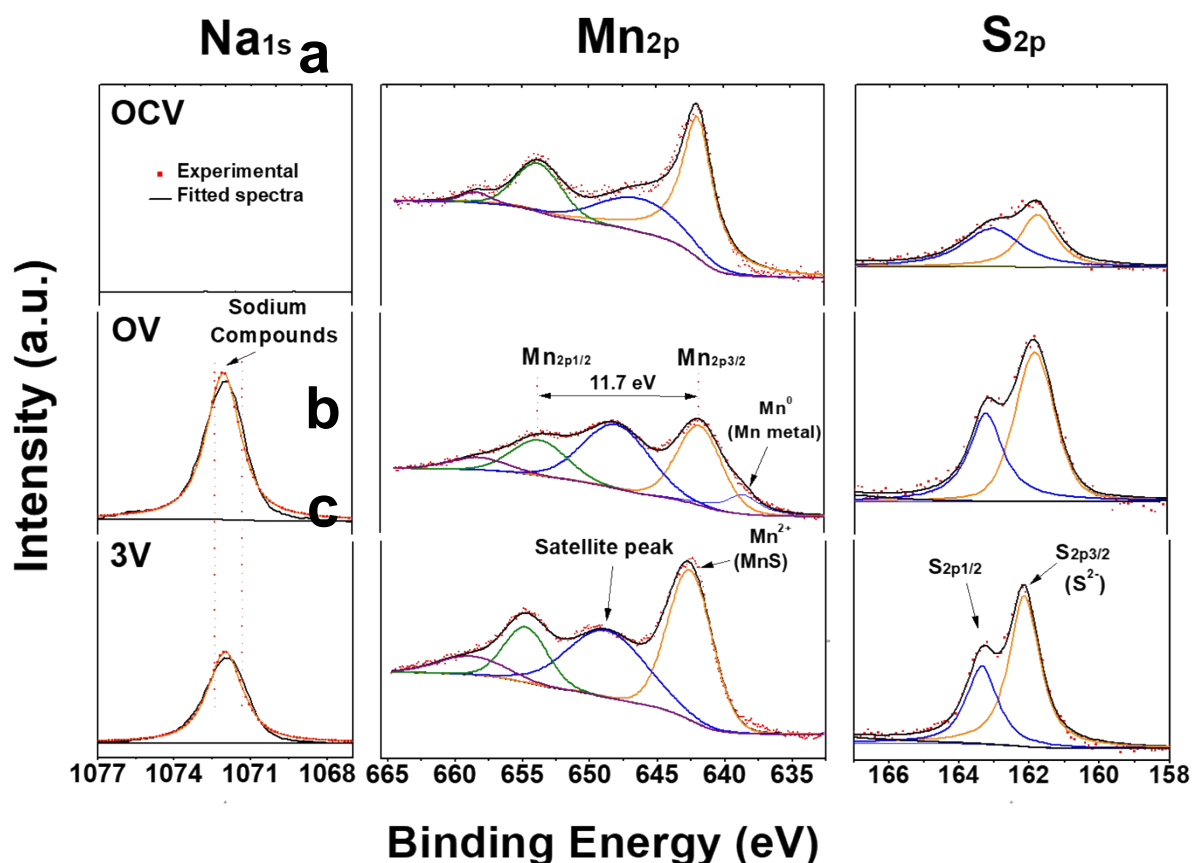


Figure S6. XPS spectra of C- α -MnS at OCV (a) 0V (b), and 3V (c): Na 1s (left), Mn 2p (center), and S 2p (right).

For the fresh electrode (marked as OCV), there is no signal related to Na (Figure S6a left). Mn2p spectrum consists of two main peaks with binding energies centering at 643.0 and 654.7 eV, which are characteristic peaks of $\text{Mn}_{2p_{3/2}}$ and $\text{Mn}_{2p_{1/2}}$, respectively. A spin-orbit splitting of 11.7 eV is consistent with the core level of Mn2p (Figure S6a center). A satellite peak indicates Mn-S-C bonds between carbon and alpha manganese sulfide [9]. And the S2p region shows a single doublet at binding energies of 162.3 eV and 163.6 eV corresponding to the $\text{S}_{2p_{3/2}}$ and $2p_{1/2}$ orbitals of S (Figure S6a right). At 0V, in Na 1s and S 2p orbitals, sodium compounds and polysulfide-related binding energies by the conversion reaction were detected (Figure S6b left and right). Strikingly the peaks related with Mn 2p orbital became broad, and there was appearance of Mn metal at 638 eV (Figure S6b center) though the relative intensity of $\text{Mn}_{2p_{3/2}}$ dramatically diminished (Figure S6b center). The relative intensity for Na was reduced after charging to 3V (Figure S6c left). Interestingly, the relative intensity of $\text{Mn}_{2p_{3/2}}$ was recovered to its original ratio of $\text{Mn}_{2p_{3/2}}$ and $\text{Mn}_{2p_{1/2}}$ at 3 V (Figure S6c center). And there is no change in the binding energy for S because of formation of MnS after desodiation to 3V (Figure S6c right).

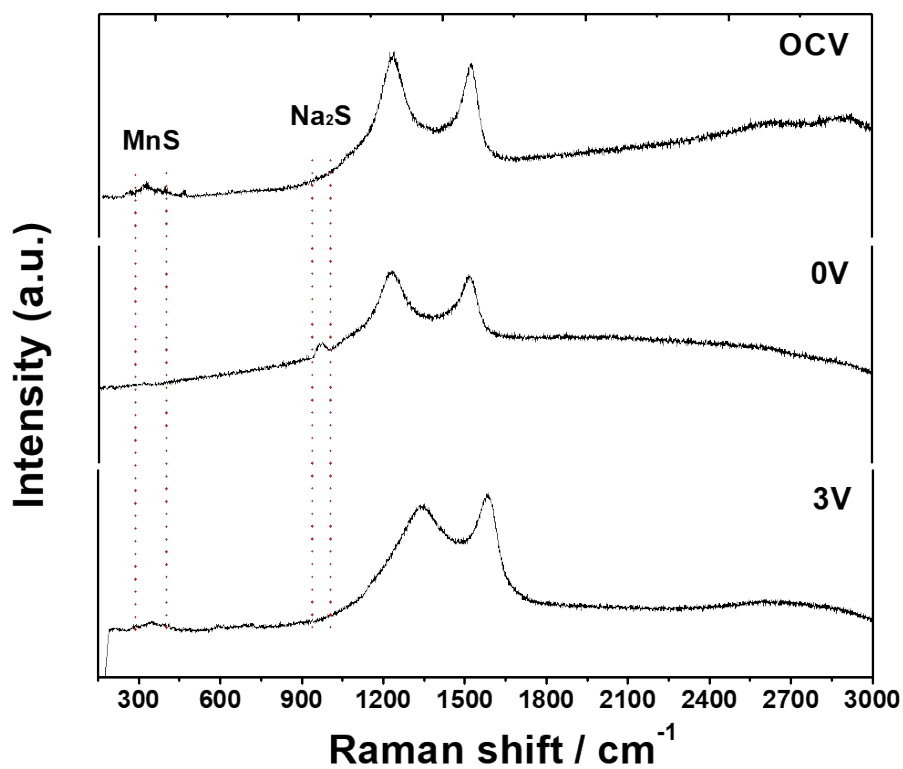

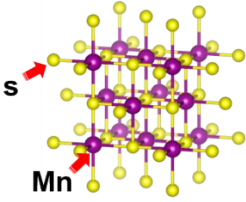

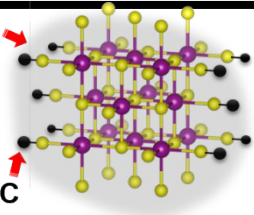

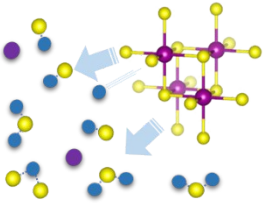

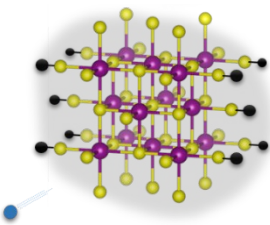


Figure S7. Raman spectra of C- α -MnS at OCV, 0V and 3V.

Since α -MnS is coated by carbon, the existence of carbon is clearly visualized at OCV, 0V and 3V after desodiated state. Note that a peak related to Na-S related peak as Na₂S [11], is clearly confirmed at 0V, while the peak is not evident after desodiation to 3V. MnS band is visible at OCV state, but the band is not clear after sodiation to 0V. Again, the MnS band revives after desodiation to 3V, validating reversibility of the conversion reaction.

Table S3. Schematic illustration for the morphological and structural evolution of bare and carbon-coated α -MnS particle upon sodiation (reduction) and de-sodiation (oxidation).

	Bare MnS		C- α -MnS	
	Morphological	Structural	Morphological	Structural
Fresh				
Post cycled				

References

- 1 X. Xu, S. Ji, M. Gu, J. Liu, ACS Appl. Mater. Interfaces, 2015, **7**, 20957.
- 2 W. Qin, T. Chen, T. Lu, D. H. C. Chua, L. Pan, J. Power Sources, 2016, **302**, 202.
- 3 Z. Li, W. Feng, Y. Lin, X. Liu, H. Fei, RSC Adv., 2016, **6**, 70632.
- 4 Y. Du, X. Zhu, X. Zhou, L. Hu, Z. Dai, J. Bao, J. Mater. Chem. A, 2015, **3**, 6787.
- 5 X. Geng, Y. Jiao, Y. Han, A. Mukhopadhyay, I. Yang, H. Zhu, Adv. Funct. Mater., 2017, **27**, 1702998.
- 6 D. Sun, D. Ye, P. Liu, Y. Tang, J. Guo, L. Wang, H. Wang, Adv. Energy Mat., 2017, **334**, 1702383.
- 7 H. He, Q. Gan, H. Wang, G.-L. Xu, X. Zhang, D. Huang, F. Fu, Y. Tang, K. Amine, M. Shao, Nano Energy, 2018, **44**, 217.
- 8 Q. Zhang, H. He, X. Huang, J. Yan, Y. Tang, H. Wang, Chem. Engineer. J., 2018, **332**, 57.
- 9 S. R. S. Kumar, M. N. Hedhili, H. N. Alshareef, S. Kasiviswanathan, Applied Physics Lett., 2010, **97**, 111909.
- 10 B. V. Crist, XPS Reports, 2009, **1**, 1
- 11 P. K. Jha, O. P. Pandey, K. Singh, J. Non-crystalline Solids, 2013, **379**, 89.